SHORT RAYLEIGH LENGTH FREE ELECTRON LASER SIMULATIONS IN EXPANDING COORDINATES

R. L. Armstead, W.B. Colson, and J. Blau
Physics Department, Naval Postgraduate School
333 Dyer Road, Monterey, CA 93943

Abstract

For compact short-Rayleigh length free electron lasers (FELs), the area of the optical beam can be thousands of times greater at the mirrors than at the beam waist. A fixed numerical grid of sufficient resolution to represent the narrow mode at the waist and the broad mode at the mirrors would be prohibitively large. To accommodate this extreme change of scale with no loss of information, we employ a coordinate system that expands with the diffracting optical mode. The simulation using the new expanding coordinates has been validated by comparison to analytical cold-cavity theory, and is now used to simulate short-Rayleigh length FELs.

INTRODUCTION

A short-Rayleigh length optical cavity may give several advantages for a high-power FEL, including reduced mirror damage and improved beam quality [1]. However, such a design poses difficult numerical problems. Since the mode area expands within the cavity many thousands of times, a very large grid is required to accurately represent the mode at both the waist and the mirrors. For example, assume a Rayleigh length of $z_0 = 0.1$ and a cavity length of $S = 30$, both normalized to the undulator length, L. Then the mode radius will expand by a factor of $(1 + (S/2)^2/z_0^2)^{1/2} = 150$. If we assume 100 gridpoints in each dimension are needed to accurately represent the mode at the waist, then 15000 gridpoints are needed at the mirrors. A two-dimensional complex, double-precision array of that size requires about 4 GB of RAM, beyond the limits of many computers. Furthermore, the simulation runtime increases as the square of the number of gridpoints. For the typical parameters given above, we estimate it would require about 4 hours for each pass through the optical cavity, running a three-dimensional simulation in (x, y, t) on a 2 GHz IBM G5 processor. For some sets of parameters, several hundred passes are needed to reach steady-state operation, implying that the program would take many weeks to run. Furthermore, if we wish to include a 4th dimension in the simulation (z) to study longitudinal modes and pulse effects, we would need at least 100 slices in the z direction. In addition, steady-state in 4D requires thousands of passes. The memory requirements would then grow to 100's of GB and the simulation runtime would increase to many years. One solution to this numerical problem is to abandon a fixed Cartesian grid, and instead use a coordinate system that expands with the diffracting optical mode. This approach [2], [3] is explained below for the FEL.

PARAXIAL EQUATION

As usual, the equation to be solved for the complex electric field a is the paraxial wave equation expressed in dimensionless coordinates,

$$[\partial_x^2 + \partial_y^2 - (4/i)\partial_\tau]a(x, y, \tau) = 0. \quad (1)$$

The dimensionless coordinates x, y, and τ are, in terms of the dimensioned coordinates X, Y, and Z: $x \equiv X(\pi/\lambda L)^{1/2}, y \equiv Y(\pi/\lambda L)^{1/2}$, and $\tau \equiv Z/L$,where L is some characteristic length (which in FEL simulations will be the undulator length), and λ is the optical wavelength. The paraxial equation follows from the usual four-dimensional second-order partial differential wave equation on the assumption that deviations from plane-wave behavior in the longitudinal (Z axis) direction are slow, a reasonable condition for a laser. Eq. 1 has been studied extensively [4], and is solved reliably by the application of an FFT, except for the numerical difficulty of the expanding beam due to diffraction.

Adopting the convention that a subscript in x, y, or τ stands for the derivative with respect to that variable, Eq. 1 becomes

$$a_{xx} + a_{yy} - (4/i)a_\tau = 0. \quad (2)$$

TRANSFORMING THE COORDINATES

In order to see the motivation for a coordinate transformation, consider the exact fundamental-mode solution to Eq. 2:

$$a(x, y, \tau) = a_0(\pi z_0/A)^{1/2} \exp(-\pi r^2/A)e^{i\phi}, \quad (3)$$

where z_0 is the dimensionless Rayleigh length Z_0/L, and where the dimensionless beam area is

$$A = \pi z_0[1 + \tau^2/z_0^2], \quad (4)$$

so that the $1/e$ beam radius is

$$w = w_0[1 + \tau^2/(z_0)^2]^{1/2}, \quad (5)$$

where $w_0 = {z_0}^{1/2}$, and

$$\phi(r, \tau) = -\arctan(\tau/z_0) + \pi r^2\tau/(Az_0). \quad (6)$$

Thus, for the case that $\tau \gg z_0$, $A \approx \pi\tau^2/z_0$ and $\phi \approx -\pi/2 + r^2/\tau$, so that

$$a(r,\tau) \approx a_0(z_0/\tau)\exp(-r^2 z_0/\tau^2)\exp(ir^2/\tau) \quad (7)$$

to within a constant phase factor. It is clear from Eq. 7 that for large τ the radius of the beam expands linearly with τ, which suggests that we define the new "expanding" independent variables by

$$x' \equiv z_0^{1/2} x/\tau, \quad (8)$$

$$y' \equiv z_0^{1/2} y/\tau, \quad (9)$$

and a new dependent variable $v(x', y', \tau')$ such that

$$a(x,y,\tau) = (1/\tau)v(x',y',\tau')\exp(ir^2/\tau), \quad (10)$$

where $r^2 \equiv x^2 + y^2$.

The phase factor $\exp(ir^2/\tau)$ characterizing an expanding spherical wave, as well as the spherical amplitude expansion factor $1/\tau$, are explicitly factored out from a, so the remaining function v has to account only for the small diffraction effects not contained in the solution for the Gaussian fundamental mode. In addition, the inverse dependence of x' and y' on τ means that the dimensions of the primed numerical grid decrease with increasing τ, i.e. in precisely the region where the physical beam (represented on the unprimed grid x and y) becomes large by diffraction.

Then some algebra, outlined below, shows that $v(x', y', \tau')$ itself does indeed satisfy exactly the same paraxial wave equation as does $a(x, y, \tau)$.

First, evaluate $a_x = (v_{x'}x'_x/\tau + i2xv/\tau^2)\exp(ir^2/\tau)$, by the chain rule applied to Eq. 10. But $x'_x = z_0^{1/2}/\tau$ by Eq. 8. So $a_x = (v_{x'}z_0^{1/2}/\tau^2 + i2xv/\tau^2)\exp(ir^2/\tau)$. One more derivative with respect to x yields

$$a_{xx} = \exp(ir^2/\tau)[v_{x'x'}z_0/\tau^3 + i4v_{x'}z_0^{1/2}x/\tau^3 + i2v/\tau^2 - 4vx^2/\tau^3]. \quad (11)$$

In the same fashion, we find that

$$a_{yy} = \exp(ir^2/\tau)[v_{y'y'}z_0/\tau^3 + i4v_{y'}z_0^{1/2}y/\tau^3 + i2v/\tau^2 - 4vy^2/\tau^3]. \quad (12)$$

Furthermore,

$$a_\tau = \exp(ir^2/\tau)[v_{x'}x'_\tau/\tau + v_{y'}y'_\tau/\tau + v_{\tau'}\tau'_\tau/\tau - v/\tau^2 - ir^2 v/\tau^3]. \quad (13)$$

Substituting Eqs. 11, 12, and 13 into Eq. 2 yields

$$v_{x'x'} + v_{y'y'} = 4\tau^2 v_{\tau'}\tau'_\tau/(iz_0). \quad (14)$$

This can be written as the paraxial wave equation in the primed coordinates,

$$v_{x'x'} + v_{y'y'} - (4/i)v_{\tau'} = 0, \quad (15)$$

if $\tau'_\tau = z_0/\tau^2$. Integrating this first order differential equation for τ' with respect to τ yields

$$\tau' = z_0[1/\tau_1 - 1/\tau], \quad (16)$$

where the constant of integration is written z_0/τ_1 so that $\tau' = 0$ when $\tau = \tau_1$. The well-understood FFT method may then be applied to Eq. 15, without the numerical difficulty of following a rapidly-expanding wavefront.

The solution for the optical field a in the near field ($\tau < \tau_1$) is calculated in the conventional coordinates x, y, and τ, then connected (using Eq. 10) onto the expanding-coordinate solution in the far field ($\tau \geq \tau_1$). Remember that $\tau = \tau_1$ corresponds to $\tau' = 0$.

Notice that for the special case of the fundamental mode in expanding coordinates,

$$v(r', \tau') = (a_0 z_0)\exp[-(r')^2], \quad (17)$$

which is independent of τ'. This trivial outcome will not apply when the fundamental mode is modified by the presence of electrons in the FEL, but does provide an opportunity to compare a numerical simulation to an exact solution. In the simulation of an actual FEL, there may be a mixture of modes rather than just the fundamental mode, but the transformation can handle the general case as well with no modification.

The schematic representations in Fig. 1 and Fig. 2 show $|a|$ expanding as a function of τ and $|v|$ as a function of τ' respectively, to illustrate the effect of the coordinate transformation. In an actual numerical simulation, we calculate $|a|$ in the region $\tau = 0$ to $\tau = \tau_1$ in (x, y, τ), then switch to the primed system (x', y', τ') to calculate $|v|$ for $\tau > \tau_1$, corresponding to $\tau' > 0$. Then we apply the transformation to recover $a(\tau)$ for $\tau > \tau_1$. The dashed lines in the diagrams remind us of the relative size of the integration steps in the primed and unprimed systems.

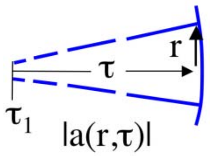

Figure 1: Contours of constant optical field amplitude $|a|$ as a function of Cartesian coordinates (r, τ) for free-space diffraction of a spherical wavefront.

In terms of the numerical integration using the expanding coordinates, constant time steps $\Delta\tau'$, correspond to time steps in the unprimed coordinates which increase quadratically with τ, so that $\Delta\tau = \tau^2\Delta\tau'/z_0$. This is a consequence of the Eq. 16, and the effect shows clearly in the progression of integration "slice" size in Fig. 3.

FREE-SPACE DIFFRACTION

The upper left picture in Fig. 3 shows a cross-section of the optical field amplitude $|a|$ in terms of the unprimed co-

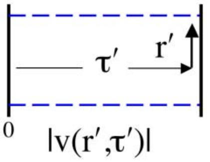

Figure 2: Contours of constant virtual field amplitude $|v|$ as a function of expanding coordinates (r', τ') for free-space diffraction of a spherical wavefront.

ordinates (x, τ) as τ goes from 0 to 3 with $\tau_1 = 1$, for the propagation of a spherical wavefront in free space. The color scale, shown in the lower-right, goes from blue (small amplitude) to yellow (large amplitude). Integration for τ between 0 and 1 is performed in the conventional coordinate τ in ten steps with $\Delta\tau = 0.1$. The interval $\tau = 1 \rightarrow 3$ corresponds to expanding coordinate $\tau' = 0 \rightarrow 0.2$. This is also integrated in ten equal steps, with $\Delta\tau' = 0.02$, and is displayed in the lower picture as the "virtual" field amplitude $|v|$ in the primed coordinates. In this calculation the Rayleigh length $z_0 = 0.3$ corresponds to initial waist size $w_0 = z_0^{1/2} \approx 0.55$. Notice that the virtual field amplitude $|v|$ appears not to change with τ' for the fundamental mode, which is precisely what Eq. 17 predicts. Also note that, compared to τ, the range of τ' is much diminished by the transformation Eq. 16. The optical field a for $\tau \geq \tau_1 = 1$ is then given in terms of the transformation Eqs. 8, 9, 16, and 10. The ratio of the beam area at $\tau = 3$ to the beam area at the waist is 100.

The right-hand pictures in Fig. 3 are both end-on cross-sections at $\tau = 3$. The upper is the optical field amplitude $|a(x, y)|$, and the lower is the virtual field amplitude $|v(x', y')|$, also at $\tau = 3$, corresponding to $\tau' = 0.2$.

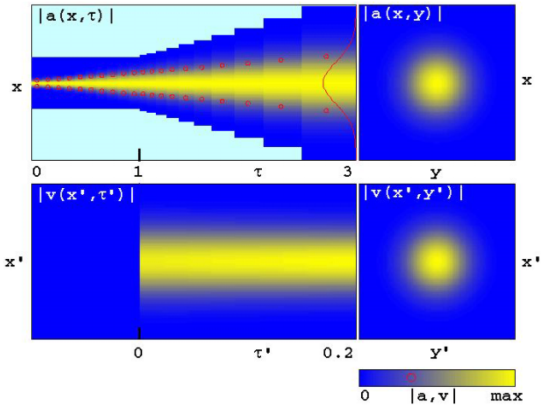

Figure 3: Free-space diffraction of a fundamental Gaussian mode in Cartesian coordinates $|a(x, \tau)|$ (top), and expanding coordinates $|v(x', \tau')|$ (bottom) for $z_0 = 0.3$, $\tau_1 = 1$, and $\tau = 0 \rightarrow 3$.

LARGER RANGE

Another calculation, shown in Fig. 4, spans a much larger range, $\tau = 0 \rightarrow 30$, with $z_0 = 0.1$. Conventional coordinates are used for for $\tau = 0 \rightarrow 1$ and primed coordinates for $\tau = 1 \rightarrow 30$, for which $\tau' = 0 \rightarrow 0.1$. Ten equal steps $\Delta\tau'$ suffice to take the field all the way to $\tau = 30$ and preserve its Gaussian shape. The ratio of the beam area at $\tau = 30$ to that at its waist is $(1 + 30^2/0.1^2) = 90,000$, and is much too large for integration in conventional coordinates. Using the coordinate transformation method, there are no distortions in the outcome, which is the same as the exact analytical result.

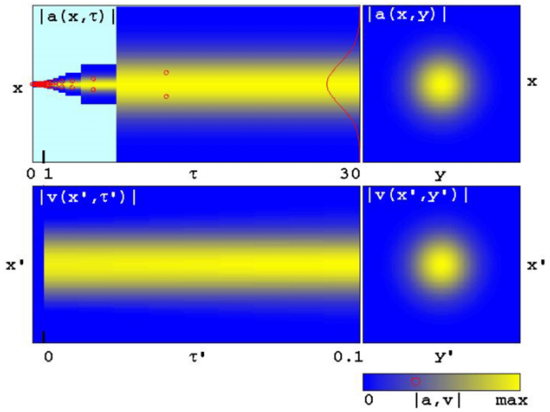

Figure 4: Free-space diffraction of a fundamental Gaussian mode in Cartesian coordinates $|a(x, \tau)|$ (top), and expanding coordinates $|v(x', \tau')|$ (bottom) for $z_0 = 0.1$, $\tau_1 = 1$, and $\tau = 0 \rightarrow 30$.

Furthermore, multiple transverse modes have been accurately propagated over this range.

ACKNOWLEDGMENTS

The authors are grateful for the support from NAVSEA, ONR, and the JTO.

REFERENCES

[1] D.W. Small, R.K. Wong, W.B. Colson, R.L. Armstead, "Free electron lasers with short Rayleigh length", Nuclear Instruments and Methods in Physics Research A393 (1997) 262.

[2] E.A. Sziklas and A.E.Siegman, "Diffraction calculations using fast Fourier transform methods,", Proc. IEEE 62, 410 (March 1974).

[3] E.A. Sziklas and A.E. Siegman, "Mode calculations in unstable resonator with flowing saturable gain. 2: Fast Fourier transform method," Appl. Opt. 14,1873-1889 (August 1975).

[4] W.H. Press et. al., "Numerical Recipes in C", 2nd Edition, Cambridge University Press, New York, 1992.